Clinical Cancer Research

Clinical Significance of PD-L1$^+$ Exosomes in Plasma of Head and Neck Cancer Patients

Marie-Nicole Theodoraki[1,2,3], Saigopalakrishna S. Yerneni[4], Thomas K. Hoffmann[3], William E. Gooding[5], and Theresa L. Whiteside[1,2,6]

Abstract

Purpose: The microenvironment of head and neck squamous cell carcinomas (HNSCC) is highly immunosuppressive. HNSCCs expressing elevated levels of PD-L1 have especially poor outcome. Exosomes that carry PD-L1 and suppress T-cell functions have been isolated from plasma of patients with HNSCC. The potential contributions of PD-L1$^+$ exosomes to immune suppression and disease activity are evaluated.

Experimental Design: Exosomes isolated from plasma of 40 HNSCC patients by size exclusion chromatography were captured on beads using anti-CD63 Abs, stained for PD-1 and PD-L1 and analyzed by flow cytometry. The percentages and mean fluorescence intensities (MFI) of PD-L1$^+$ and PD-1$^+$ exosome/bead complexes were correlated with the patients' clinicopathologic data. PD-L1^{high} or PD-L1^{low} exosomes were incubated with activated CD69$^+$ human CD8$^+$ T cells ± PD-1 inhibitor. Changes in CD69 expression levels on T cells were measured. Patients' plasma was tested for soluble PD-L1 (sPD-L1) by ELISA.

Results: Levels of PD-L1 carried by exosomes correlated with patients' disease activity, the UICC stage and the lymph node status ($P = 0.0008$–0.013). In contrast, plasma levels of sPD-L1 or exosome PD-1 levels did not correlate with any clinicopathologic parameters. CD69 expression levels were inhibited ($P < 0.03$) by coincubation with PD-L1^{high} but not by PD-L1^{low} exosomes. Blocking of PD-L1$^+$ exosome signaling to PD-1$^+$ T cells attenuated immune suppression.

Conclusions: PD-L1 levels on exosomes, but not levels of sPD-L1, associated with disease progression in HNSCC patients. Circulating PD-L1$^+$ exosomes emerge as useful metrics of disease and immune activity in HNSCC patients. Significance: Circulating PD-L1^{high} exosomes in HNC patients' plasma but not soluble PD-L1 levels associate with disease progression. *Clin Cancer Res; 24(4); 896–905. ©2017 AACR.*

Downloaded from http://aacrjournals.org/clincancerres/article-pdf/24/4/896/2049722/896.pdf by guest on 21 May 2025

Introduction

The tumor microenvironment (TME) of head and neck squamous cell carcinomas (HNSCC) is known to be highly immunosuppressive and is characterized by the excessive production of various inhibitory factors, which interfere with antitumor immune responses (1–3). Despite various treatment regimens currently available for HNSCC, the 5-year overall survival of patients with advanced tumors has not improved in the last decade, remaining at approximately 50%, with treatment failures largely due to locoregional recurrences (4). It has been suggested that ineffective antitumor immune responses in patients with advanced HNSCC contribute to tumor progression and poor outcomes (1).

Among various immunosuppressive mechanisms operating in HNSCC, the PD-1/PD-L1 pathway has recently been of special interest. The PD-1 receptor is an immune checkpoint that limits activity of immune cells in the peripheral tissues, and thus prevents tissue damage. PD-1 is expressed on nearly all types of immune cells, and its signaling in CD8$^+$ T cells directly inhibits effector T-cell functions, including proliferation, survival, cytokine production, and cytotoxicity (5, 6). PD-1 binds two ligands, PD-L1 and PD-L2, which are broadly distributed among immune as well as nonhematopoietic cells (7). Although PD-L2 expression is restricted to immune cells, tumor cells are often PD-L1$^+$, and PD-L1 expression levels in various tumor types have been associated with poor prognosis (8). In the context of tumor progression, PD-L1 presence on the surface of tumor cells drives immune suppression and contributes to tumor immune escape (9). PD-L1–driven suppression may be reversed by immune checkpoint inhibition with anti–PD-1 or anti–PD-L1 Abs (10). Immune checkpoint inhibition has emerged as a promising anticancer strategy for many different tumor types, including HNSCC (11, 12). Nevertheless, many cancer patients do not benefit from this immunotherapy (11). In HNSCC the response rate has been reported to be approximately 15% (11). The reasons for this low response rate are unclear, but it is likely that either the mechanisms responsible for PD-L1–driven signaling are not fully understood or that other immunosuppressive pathways operating in the TME account for poor patient outcome.

[1]Department of Pathology, University of Pittsburgh School of Medicine, Pittsburgh, Pennsylvania. [2]UPMC Hillman Cancer Center, Pittsburgh, Pennsylvania. [3]Department of Otorhinolaryngology, Head and Neck Surgery, University of Ulm, Ulm, Germany. [4]Department of Biomedical Engineering, College of Engineering, Carnegie Mellon University, Pittsburgh, Pennsylvania. [5]Biostatistics Facility, UPMC Hillman Cancer Center, Pittsburgh, Pennsylvania. [6]Departments of Immunology and Otolaryngology, University of Pittsburgh School of Medicine, Pittsburgh, Pennsylvania.

Note: Supplementary data for this article are available at Clinical Cancer Research Online (http://clincancerres.aacrjournals.org/).

Corresponding Author: Theresa L. Whiteside, University of Pittsburgh Cancer Institute, Hillman Cancer Center Research Pavilion, 5117 Centre Avenue, Room 2.26b, Pittsburgh, PA 15213. Phone: 412-624-0096; Fax: 412-624-0264; E-mail: whitesidetl@upmc.edu

doi: 10.1158/1078-0432.CCR-17-2664

©2017 American Association for Cancer Research.

Translational Relevance

The PD1/PD-L1 axis has been a target of cancer immunotherapy with immune checkpoint inhibitors. Attenuation of its immunosuppressive effects improves outcome for many but not all cancer patients. Currently, PD-L1 expression by the tumor is viewed as a prerequisite for anti–PD-L1 Ab therapy. Here, we report that plasma-derived exosomes in patients with HNSCC carry biologically active PD-L1, which induces T-cell dysfunction upon coincubation of these exosomes with activated CD8$^+$ T cells. Although levels of soluble PD-L1 (sPD-L1) were elevated in patients' plasma, only exosome-bound PD-L1 levels correlated with disease activity and with the patients' clinicopathologic profiles. Anti–PD-1 Abs reversed suppression induced by PD-L1$^+$ exosomes in activated T cells. Circulating PD-L1$^+$ exosomes emerge as promising potential markers of immune dysfunction and disease progression in patients with HNSCC.

Tumor-derived exosomes (TEX) have recently captured attention as regulatory elements through which cancer cells can communicate with and reprogram the immune cells populating in the TME (13). TEX are nano-sized (30–150 nm) vesicles that originate in the endosomal compartment of parent cells and transfer inhibitory receptor/ligands and nucleic acids from the tumor to recipient cells (14, 15). Tumors, including HNSCC, are avid TEX producers, and plasma of cancer patients is enriched in TEX (16). To date, studies of TEX, largely performed with tumor cell line–derived exosomes, have demonstrated that these exosomes represent an effective mechanism of immunosuppression (17, 18). Exosomes isolated from plasma of HNSCC patients are also strongly immunosuppressive and, as we have recently demonstrated, play a role in the regulation of tumor progression (16). Interestingly, these exosomes were shown to carry PD-L1 and PD-1 (16). It is not clear, however, whether PD-1 and PD-L1 carried by these exosomes are biologically active and represent proteins responsible, in part, for the reported immunoinhibitory effects and clinical correlations (16).

Here, we test the hypothesis that PD-1 and PD-L1 carried on exosomes isolated from plasma of HNSCC patients have a significant impact on: (i) disease progression and (ii) immune cell functions in patients with HNSCC. Our data indicate that PD-L1 carried on exosomes, but not serum levels of soluble PD-L1, correlate with disease activity, and that blocking of exosome signaling to T cells with anti–PD-1 Abs effectively attenuates immune suppression mediated by the PD-L1$^+$ exosomes.

Materials and Methods

Patients

Peripheral blood specimens were randomly obtained from 40 HNSCC patients seen at the UPMC Otolaryngology Clinic between years 2004 and 2016. The collection of blood samples and access to clinical data for research were approved by the Institutional Review Board of the University of Pittsburgh (IRB #960279, IRB #0403105, and IRB #0506140). Table 1 provides clinicopathologic characteristics of the patients enrolled in the study. The blood samples were delivered to the laboratory and were centrifuged at 1,000 × *g* for 10 minutes. Plasma specimens were stored in 1-mL aliquots at −80°C and were thawed immediately prior exosome isolation.

Table 1. Clinicopathologic parameters of HNSCC patients who participated in the study

Clinicopathologic data	Patients ($n = 40$) *n* (%)
Age, y	
≤61	13 (32.5)
>61	27 (67.5)
(range, 26–78)	
Gender	
Male	31 (77.5)
Female	9 (22.5)
Disease status	
AD	23 (57.5)
NED	17 (42.5)
Primary tumor site	
Oral cavity	20 (50)
Pharynx	10 (25)
Larynx	9 (22.5)
Other localization	1 (2.5)
Tumor stage	
T1	12 (30)
T2	12 (30)
T3	10 (25)
T4	6 (15)
Nodal status	
N0	18 (45)
N1	7 (17.5)
N2	11 (27.5)
N3	4 (10)
Distant metastasis	
M0	40 (100)
UICC stage	
I	14 (35)
II	7 (17.5)
III	13 (32.5)
IV	6 (15)
HPV status (p16 IHC)	
Positive	8 (20)
Negative	11 (27.5)
Undefined	21 (525)
Alcohol consumption	
Yes	25 (62.5)
No	13 (32.5)
Unknown	2 (5)
Tobacco consumption	
Yes	28 (70)
No	11 (27.5)
Unknown	1 (2.5)

Exosome isolation by mini size-exclusion chromatography

The mini size-exclusion chromatography (mini-SEC) method for exosome isolation was established and optimized in our laboratory as described previously (ref. 18; EV-TRACK ID: EV160007). Briefly, plasma samples were thawed and were centrifuged first at 2,000 × *g* for 10 minutes at room temperature and then for 30 minutes at 10,000 × *g* at 4°C. Next, plasma was ultrafiltered using a 0.22-μm filter (EMD Millipore). An aliquot of plasma (1 mL) was placed on a mini-SEC column and eluted with PBS. The fourth 1-mL void volume fraction enriched in exosomes was collected. The fraction #4 contained the majority of isolated exosomes as reported previously (18).

Downloaded from http://aacrjournals.org/clincancerres/article-pdf/24/4/896/2049722/896.pdf by guest on 21 May 2025

Characteristics of plasma-derived exosomes

Exosomes isolated by mini-SEC were evaluated for their size by qNano (Izon), morphology by transmission electron microscopy, and cellular origin by Western blots to confirm the presence of endosomal markers (e.g., TSG101) as described previously (16).

BCA protein assay and exosome concentration

The protein concentration of the isolated exosome fraction #4 was determined using a Pierce BCA protein assay kit (Pierce Biotechnology), according to the manufacturer's instructions. Exosomes were concentrated using Vivaspin 500 (VS0152, 300,000 MWCO, Sartorius). For FACS analysis, 10 μg of protein in 100 μL of PBS were used.

Flow cytometry for detection of surface proteins on exosomes

For flow cytometry of exosomes coupled to beads, the method described by Morales–Kastresana (19) was modified as follows:

Exosome capture on magnetic beads. For detecting exosome-associated surface proteins by flow cytometry, exosomes were first captured on ExoCap Streptavidin magnetic beads (Supplementary Fig. S1A) purchased from MBL International. Exosomes (10 μg/100 μL PBS in 0.5-mL Eppendorf microfuge tubes) were coincubated with biotin-labeled anti-CD63 mAb (clone 353018 from Biolegend) adjusted to the concentration of 1 μg for 2 hours at room temperature. Next, a 10-μL aliquot of beads was added and the tubes were again incubated for 2 hours at room temperature. Samples were washed 1 with dilution buffer from the kit using a magnet. The bead/anti-CD63Ab/exosome complexes were then coincubated with the labeled detection Abs, either anti-PD-L1 PE (12-5983-42) or anti-PD-1 PE (12-2799-42) or with the labeled isotype control Ab for 1 hour at room temperature. The Abs were purchased from eBioscience. Next, the complexes were washed 3× using a magnet and were resuspended in 300 μL of PBS for antigen detection by flow cytometry.

Preliminary titrations of the capture mAb. The optimal ratio of anti-CD63 mAb: exosome protein: beads used for capture was determined in preliminary experiments. Titrations were first set up with different protein concentrations of exosomes (5, 10, and 20 μg); of anti-CD63 mAb (0.1–2.0 μg) and different volumes of beads (10–150 μL). The concentrations/volumes that gave the highest percentage values and mean fluorescence intensities (MFI) for PD-L1 or PD-1 upon detection by flow cytometry were: 10 μg exosome protein, 0.5 μg of anti-CD63 mAb per 50 μL of PBS and 10 μL of beads. Using these conditions, capture of exosomes with the isotype control Ab gave negative results. Once the optimal capture conditions for anti-CD63 mAb were determined, they were routinely used in all subsequent experiments. To evaluate the efficiency of this exosome capture method, the uncaptured exosomal fraction (after the removal of exosome/Ab/bead complexes using a magnet) was collected and recaptured with anti-CD63 mAb (Supplementary Fig. S1B). Supplementary Table S1 shows the results of 3 patients with consistent high CD63 exosome levels in the captured fraction and very few $CD63^+$ exosomes in the uncaptured fraction. The detection with anti-PD-1 or anti-PD-L1 mAbs was performed as described below.

Flow cytometry–based detection of exosomes. The flow cytometry of exosomes captured on beads for detection of antigens carried on the exosome surface is illustrated in Supplementary Fig. S1B. In preliminary titration experiments, different concentrations (0.625–5.0 μg) of the fluorochrome-conjugated detection Abs and isotype controls were coincubated with 10 μg of exosome protein and 10 μL of beads to determine the optimal conditions for staining and detection of PD-1 and PD-L1 carried by captured exosomes. The isotype control was used according to the manufacturer's instructions and had the same concentration as the test Ab. The optimal Ab concentration (0.5 μg) that gave the highest separation index between the detection Ab and isotype control (MFI_1-$MFI_2/[\sqrt{(SD_1+SD_2)/2}]$) upon flow cytometry was selected for all experiments. Detection was performed immediately after staining using the Gallios flow cytometer equipped with Kaluza 1.0 software (Beckman Coulter). Samples were run for 2 minutes and around 10,000 events were acquired. Gates were set on the bead fraction visible in the forward/sideward light scatter.

Exosomes obtained from plasma of all 40 HNSCC patients were analyzed by flow cytometry. The lower edge of the "positive" gate was set at the point where <2% of the isotype control was positive (approximately 2 SD from the isotype mean; see Supplementary Fig. S5). Percent positive beads were measured as well as MFI. ΔMFIs were calculated by subtracting the isotype control MFI from the sample MFI. Results are presented as percent positive values or relative fluorescence values (RFV), where the RFV = % positive beads × ΔMFI of beads loaded with $CD63^+$ exosomes captured from fraction #4. RFVs were calculated for $PD\text{-}L1^+$ and $PD\text{-}1^+$. All data are normalized to 1-mL plasma used for exosome isolation by mini-SEC.

Reproducibility of the flow cytometry–based detection assay. Before routine application of the detection method to monitoring of plasma-derived exosomes for PD-L1, its reproducibility was validated. Exosomes isolated from plasma of 3 different HNSCC patients were divided into 3 aliquots. Each of these aliquots was divided again into 3 parts and stained for PD-L1 (the total of 3 × 9 aliquots). Results of flow cytometry (% $PD\text{-}L1^+$ exosomes) showed that the assay had excellent reproducibility with the experimental error of only 7% (Supplementary Fig. S2).

Immunostaining and imaging of exosomes captured on magnetic beads

Plasma-derived exosomes captured with anti-CD63 mAb on magnetic beads as described above were first coincubated with 10% (v/v) of normal goat serum in PBS-Tween (0.1%; PBST) at room temperature for 60 minutes to block nonspecific staining. Primary staining was performed using anti-CD63 mAb (5 μg/mL) or rabbit anti-PDL1 Ab (5 μg/mL) at 4°C overnight. Following washing ×3 with PBST, secondary staining was performed with Alexafluor 488- or Alexafluor 647-conjugated goat Abs (2 μg/mL), respectively, at 4°C overnight. Unbound Abs were removed by washing 3× with PBST using a magnet. Stained exosomes on beads were placed into compartments made on an epoxy-silane–coated glass slide by using silicone barriers (Grace Biolab). Ceramic (ferrite) disc magnets were placed under the slide to sediment the magnetic beads which were added to each compartment in 10-μL aliquots (1×10^6 beads). After 5-minute incubation at room temperature, magnets were removed, and the slide was placed in a humidified chamber at 4°C overnight, washed 3× with PBS, and fixed using 4% (v/v) paraformaldehyde (Electron Microscopy Services) for 15 minutes at room temperature. Next, the silicon barriers were stripped off the slide, which was then coverslipped using Prolong Gold Anti-fade reagent

Downloaded from http://aacrjournals.org/clincancerres/article-pdf/24/4/896/2049722/896.pdf by guest on 21 May 2025

(Invitrogen) and examined in a Zeiss LSM 880 confocal microscope (Zeiss) using oil-immersion 63× objective. Image analysis was performed using Imaris (Bitplane) and ZEN blue (Zeiss) software. To quantify fluorescence, six random pictures per compartment were captured, and the total fluorescence intensities of respective channels were measured after background correction using ImageJ software (NIH, Bethesda, MD).

Functional assays

To determine whether exosomes, which are PD-L1^{high} or PD-L1^{low} have suppressive effects on T cells, coincubation experiments were performed. PBMCs were harvested from healthy donor's buffy coats by centrifugation on Ficoll–Hypaque gradients, and CD8$^+$ T cells were separated via negative selection using AutoMAX (Miltenyi Biotec) as described previously (20). Aliquots (2×10^5) of T cells were placed in wells of 96-well plates and activated with anti-CD3/anti-CD-28 antibody–coated beads (25 μL/mL; StemCell Technologies) and IL2 (150 IU/mL) for 5–6 hours at 37°C. Exosomes (fraction #4, 50 μg protein) obtained from plasma of HNSCC patients and previously characterized for the high versus low PD-L1 content ($n = 14$), were added to T cells and incubated for 16 hours. As control, PBS was added in place of exosomes. Activated T cells were harvested and stained for CD8 using PE-labeled mAb #IM0452U) and for CD69 using FITC-labeled mAb #555530, both purchased from Beckman Coulter. Expression levels of CD69 on CD8$^+$ T cells were measured by flow cytometry. Isotype controls were included in all experiments. The gates were set on CD8$^+$ T cells, and the frequency as well as relative fluorescence intensity (MFI of Ab$^+$/MFI of Isotype) of CD69$^+$CD8$^+$ T cells were determined.

Next, anti–PD-1 Ab, #AF1086 lot #ICA02 (purchased from R&D Systems) was used to block effects of exosome-mediated suppression. CD8$^+$ T cells were either incubated with the PD-1 inhibitory Ab (30 μg/mL) or goat IgG isotype control for 1 hour after IL2/CD3/CD28 activation for 5–6 hours at 37°C. Next, PD-L1^{high} or PD-L1^{low} exosomes (50 μg) were added and incubated with CD8$^+$ T cells for 16 hours ($n = 5$). Surface expression levels of CD69 on CD8$^+$ T cells were monitored by flow cytometry.

Detection of soluble PD-L1

For the detection of soluble PD-L1 in patients' plasma, a commercially available the ELISA Kit was used (Abcam, #ab214565). Plasma samples of 37 HNSCC patients were prepared and tested according to the manufacturer's specifications manual. Samples and standards were measured in duplicates.

Statistical analysis

Statistical analysis was performed using GraphPad Prism (version 7, GraphPad Software). Scatter plots depict means and SEM. When data are presented as box plots, the bar indicates the median, the box shows the interquartile range (25%–75%) and the whiskers extend to 1.5× the interquartile range. The Kruskal–Wallis test was used for group comparisons. Spearman correlation coefficient was used to identify correlations between groups. To determine reproducibility of the detection method, interclass correlation coefficients were calculated. The standard error of measurement was used to determine the 95% prediction intervals. Exosome levels were also compared across 4 patient groups defined by both the stage and disease status with a one-way ANOVA. Pairwise contrasts were tested by the Turkey HSD method. The P value of <0.05 was used to evaluate significance of the data.

Results

Clinicopathologic characteristics of HNSCC patients

The clinicopathologic characteristics of the patients are listed in Table 1. The patients' mean age was 61 years, and they were predominantly male. Anatomic locations of the primary tumors were: the oral cavity (50%), the pharynx (25%), and the larynx 22.5%). Twenty-three patients (57%) donated blood at the time of diagnosis before any therapy. These patients had an active disease (AD). Seventeen patients (42%) donated blood after completing curative therapy at the time when they had no evidence of disease (NED) as determined by clinical evaluations. Supplementary Table S2 provides information on the treatment regimens of these patients. At diagnosis, most patients (60%) presented with an early tumor stage (T1 and T2) and 45% had a negative nodal status. No patient had distant metastases (100% M0). Half of the patients (52.5%) were UICC I or II and 47.5% were UICC III or IV. The majority of patients had a moderate histologic differentiation grade by histopathology. The HPV status, routinely determined by p16 IHC, was positive in 8 patients, negative in 11 patients but was not evaluated in 21 patients. Seventy percent of patients consumed tobacco and/or alcohol (62.5%) at the time of diagnosis. None of the patients received immune checkpoint inhibition immunotherapy.

Detection of PD-L1 on exosomes

Although the flow cytometry–based assessment of PD-L1 carried by exosomes captured with anti-CD63 mAb and bound to magnetic beads was found to be highly reproducible (Supplementary Fig. S2). Nevertheless, the comparison of this method with imaging by confocal microscopy was performed to further confirm the validity of the flow-based antigen detection on exosomes. To this end, exosome samples of 3 HNSCC patients with low, high, and intermediate content of PD-L1 were compared for relative quantities of this ligand detected by the two methods (Fig. 1). By flow cytometry, the RFVs for PD-L1 were 33, 168, and 68 for the exosomes captured on beads, respectively (Fig. 1D). By quantitative confocal imaging, relative ratios of PD-L1 MFI/CD63 MFI in these exosomes show low, high, and intermediate values that are similar to those detected by flow cytometry (Fig. 1C). These experiments show that PD-L1 levels on the exosome surface are reproducibly measured by two different methods.

Exosome protein levels correlate with disease activity in HNSCC

We have previously reported that total protein concentration of exosomes isolated from HNSCC plasma by SEC correlated with disease activity (16). Here, we have extended this finding to a larger and different patient cohort. Significantly higher ($P < 0.0005$) exosome protein levels were seen in patients with active disease than in those with NED after therapy (Fig. 2A).

Association of surface PD-L1 and PD-1 levels with clinicopathologic data

Results of detection analyses for PD-L1 and/or PD-1 content on exosomes were examined for association with the clinicopathologic data for all HNSCC patients. The data are normalized to

Downloaded from http://aacrjournals.org/clincancerres/article-pdf/24/4/896/2049722/896.pdf by guest on 21 May 2025

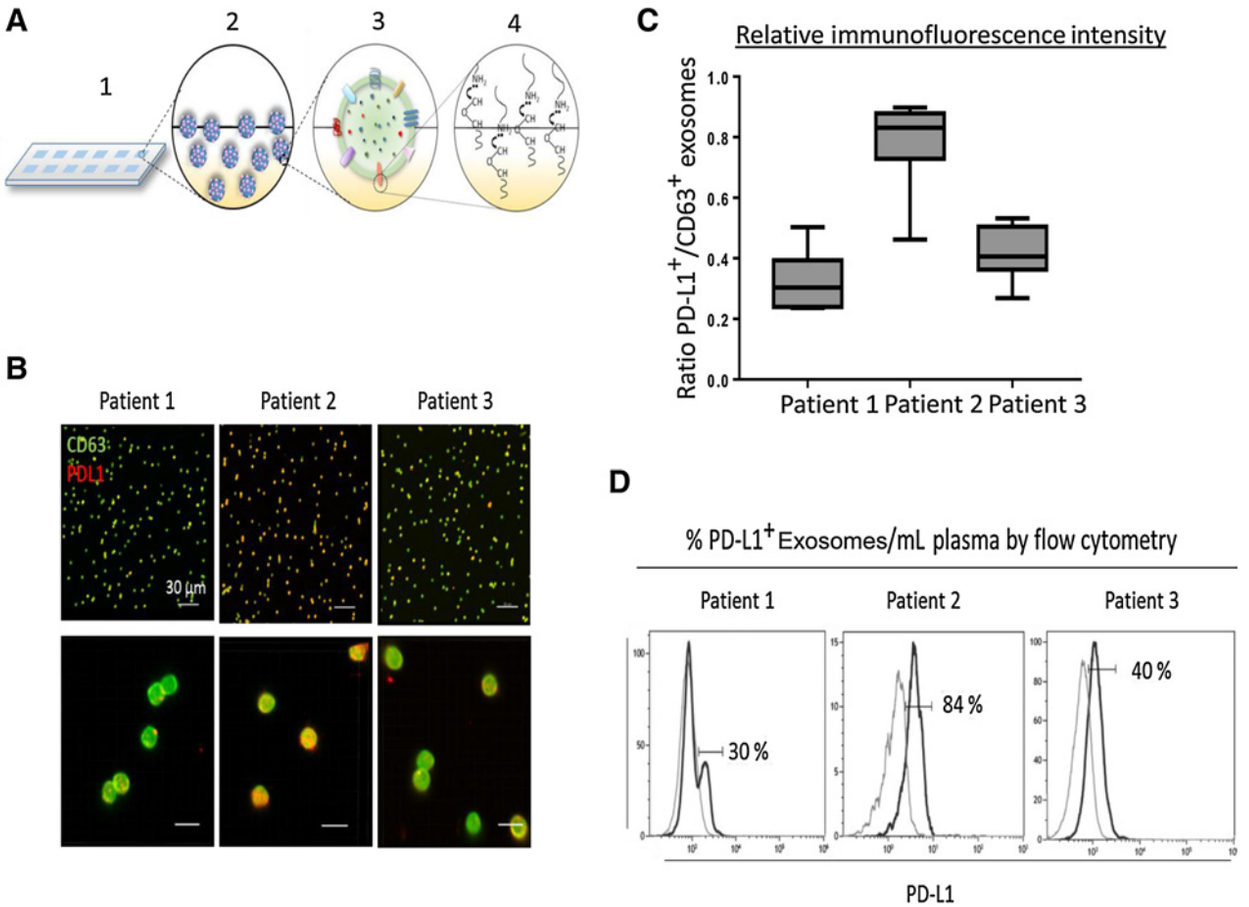

Figure 1.

Comparisons of flow cytometry with confocal microscopy imaging for detection of PD-L1 on exosomes isolated from plasma of three HNSCC patients. Exosomes were captured on beads using biotinylated anti-CD63 mAb and were then stained with labeled anti-PD-L1 mAb for detection of PD-L1 by flow cytometry or by confocal microscopy. **A,** Exosome immobilization for confocal microscopy: 1, the epoxy-silane slide; 2, exosomes are deposited into wells on the slide; 3 and 4, proteins on the surface of exosomes interact with epoxy-silane on the slide via their exposed amine-, thiol-, and hydroxyl-groups, immobilizing exosomes for confocal imaging. **B,** Confocal microscopy images of exosomes of the 3 patients. Exosomes captured on beads and immobilized on the epoxy-silane slide were stained with labeled anti-CD63 (green) and anti-PD-L1 (red) mAbs (mag ×10, top and mag ×252, bottom). Note differences in staining intensities of the exosomes for PD-L1 (low for patient #1, high for patient #2, and intermediate for patient #3). **C,** Quantification of immunofluorescence signals for the immobilized exosomes of the three HNC patients. Note that the staining intensity for PD-L1 in each patient's exosomes corresponds to the flow cytometry data (shown in **D**). **D,** The percentages for PD-L1$^+$ exosomes detected by flow cytometry are different for each patient (33, 168, and 68).

1-mL plasma used for exosome isolation for each patient by mini-SEC. As shown in Fig. 2B, significant elevation in the percentages or RFVs (not shown) for PD-L1$^+$ exosomes was observed in AD patients versus those who were NED ($P < 0.0137$). Similarly, patients with N+1 disease had significantly higher percentages or RFVs for PD-L1$^+$ exosomes in plasma than those who were N0 ($P = 0.0008$). Patients with the high UICC stage (III and IV) had higher percentages or RFVs for PD-L1$^+$ exosomes in plasma than patients who were UICC stage I/II ($P = 0.0001$). Almost identical correlation was observed for the differences between the patients with the T stage III/IV versus the T stage I/II (data not shown). No differences were seen for PD-L1 on exosomes in patients stratified by the histologic grade or anatomic side of the tumor, although a trend toward higher PD-L1 levels in poorly differentiated tumors can be suspected (see Supplementary Fig. S3).

The strength of the observed correlations was further evaluated by crossing the stage with disease activity and creating four patient groups (Fig. 3). Variation in PD-L1$^+$ exosomes was largely related to the UICC stage and less so to disease activity. The AD patients with advanced UICC stages had significantly higher RFVs for PD-L1$^+$ exosomes in plasma than the AD patients with lower UICC stages or the NED patients with higher UICC stages. The AD and NED patients with low UICC stages had comparatively low RFVs for PD-L1$^+$ exosomes. Corresponding results were obtained by crossing the disease status with lymph node involvement status (data not shown).

In contrast with PD-L1, the RFVs for PD-1 on plasma-derived exosomes (Fig. 2B) were not associated with any of the clinico-pathologic parameters. Indeed, PD-1$^+$ exosomes on beads were uniformly high in plasma of all 40 HNSCC patients. On the other hand, PD-L1$^+$ exosomes were highly variable, and no correlation between RFVs of PD-L1$^+$ versus PD-1$^+$ plasma-derived exosomes was seen in this cohort of patients (Spearman correlation, $P = 0.9$, $r = 0.005$; Fig. 4A).

Downloaded from http://aacrjournals.org/clincancerres/article-pdf/24/4/896/2049722/896.pdf by guest on 21 May 2025

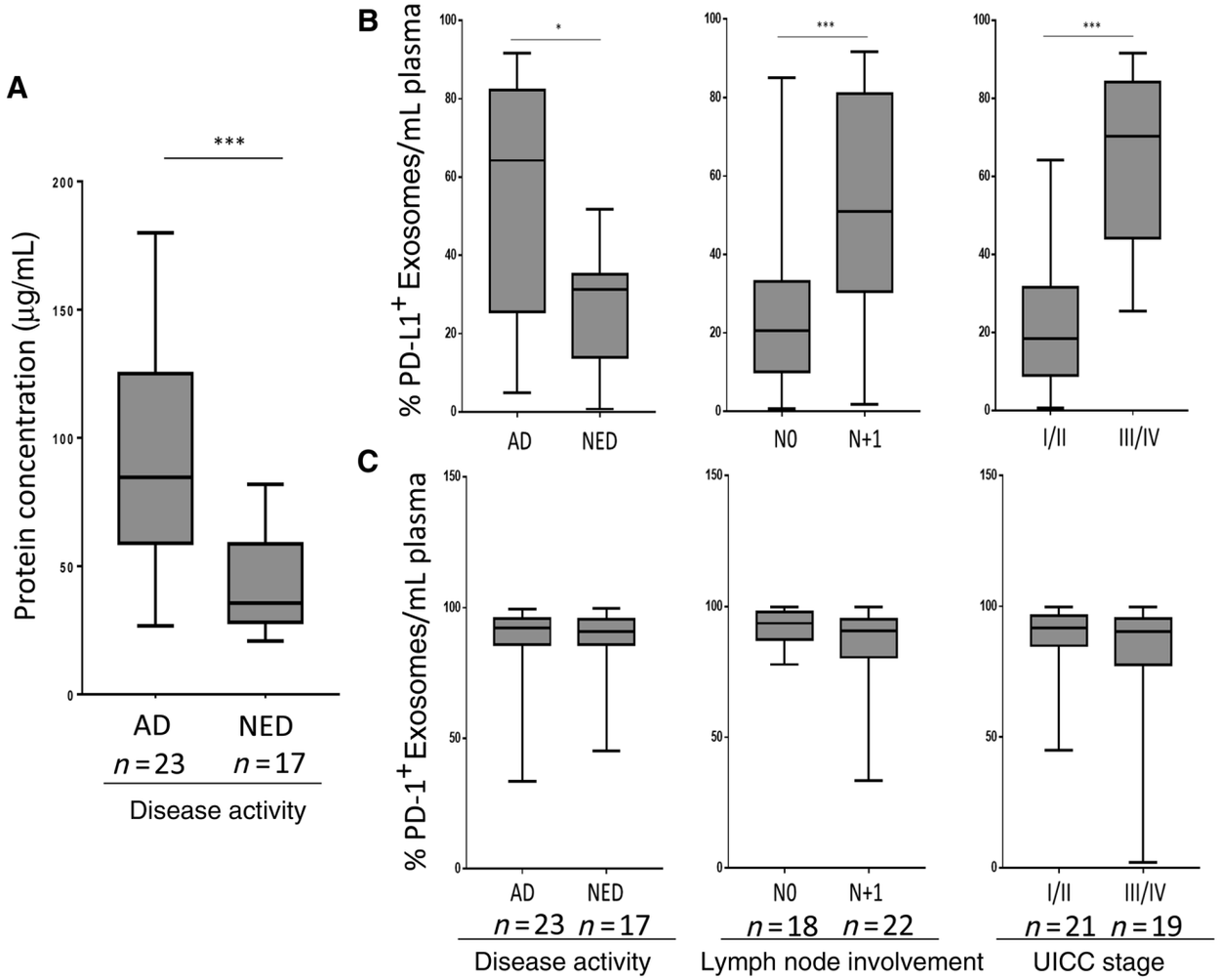

Figure 2.

Protein levels of exosomes and percentages of PD-1$^+$ or PD-L1$^+$ exosomes in plasma of patients with HNSCC. **A,** Protein concentrations of exosomes (μg/mL plasma) are significantly elevated in patients with active disease (AD) relative to those with no evidence of disease after therapy (NED); **B,** The percentages (or RFVs, not shown) for PD-L1$^+$ exosomes are significantly higher in AD patients, patients with positive lymph nodes and patients with the high (III/IV) UICC stage tumors at diagnosis. *, $P < 0.05$; ***, $P < 0.0008$. **C,** The percentages (or RFVs, not shown) for PD-1 exosomes in plasma are not statistically different in HNSCC patients stratified by disease activity, lymph node, or UICC status. The data presented as box plots are normalized to the frequency of exosomes/1 mL of patients' plasma in this and the subsequent figures.

Soluble PD-L1 does not correlate with clinicopathologic data in HNSCC

In addition to measuring the PD-L1 content in exosomes, we also studied plasma levels of soluble PD-L1 by ELISA in 38 of 40 HNSCC patients. The range of values for PD-L1 in plasma was 53.6 pg/mL ± 50.8 (the median value = 35 pg/mL). As Supplementary Fig. S4 shows, soluble PD-L1 did not correlate with clinicopathologic parameters in the patients. Furthermore, no correlation between levels of soluble PD-L1 and exosome content of PD-L1 was observed (Spearman correlation at $P = 0.85$, $r = 0.03$; Fig. 4B).

PD-L1^{high} exosomes downregulate CD69 expression on effector T cells

We have previously demonstrated that TEXs suppress T-cell activation (21). To determine whether PD-L1$^+$ exosomes isolated from plasma of HNSCC patients suppress functions of CD8$^+$ effector T cells, we activated normal human CD8$^+$ T cells and coincubated them with PD-L1^{high} or PD-L1^{low} exosomes. Upon activation via the T-cell receptor, CD8$^+$ T cells upregulated surface CD69 as well as surface PD-1 expression (Fig. 5A). Following coincubation of these T cells with PD-L1$^+$ exosomes, CD69 expression levels decreased (Fig. 5B and C), and the decrease was dependent on the exosome PD-L1 cargo. PD-L1^{high} exosomes induced significant downregulation of CD69 on T cells, while PD-L1^{low} exosomes did not (Fig. 5C). Furthermore, in the presence of anti–PD-1 Ab, downregulation of CD69 expression levels was blocked (Fig. 5D), confirming that the decrease in expression of CD69, a T-cell activation marker (22), was due to the ligation of PD-L1 carried on exosomes to PD-1 expressed on CD8$^+$ T cells. These experiments showed that PD-L1 carried on exosomes is biologically active and interferes with activation of effector T cells.

Downloaded from http://aacrjournals.org/clincancerres/article-pdf/24/4/896/2049722/896.pdf by guest on 21 May 2025

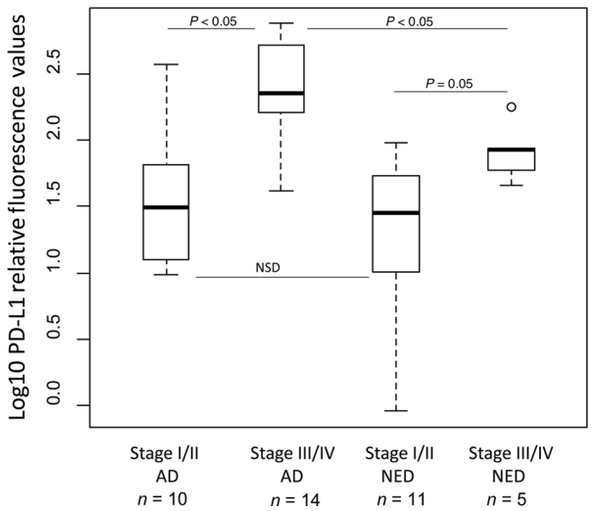

Figure 3.

RFVs for PD-L1$^+$ exosomes in plasma of patients with HNSCC stratified by disease activity and stage to create four patient groups: AD-UICC I/II, AD-UICC III/IV, NED-UICC I/II, and NED-UICC III/IV. AD patients with high UICC stage had significantly increased RFVs for PD-L1$^+$ exosomes in plasma compared with AD with low UICC stage or NED with low UICC stage.

Discussion

We have reported earlier that exosomes isolated from plasma of cancer patients carry immune checkpoint molecules, including PD-1, PD-L1, and CTLA-4 (16, 18). The presence of these proteins in the exosome cargo was detected by Western blots, and thus it was unclear whether they were carried in the exosome lumen or on the exosome membrane. It was also uncertain whether these proteins mediated immune suppression upon coincubation of exosomes with activated T cells. In this study, using flow cytometry–based detection assay for exosomes covalently bound to beads, we show that PD-1 and PD-L1 are components of exosome cargo, decorate exosome surface, and can be quantitated using labeled mAbs specific for the receptor or the ligand. Interestingly, our earlier studies using semiquantitative Western blots suggested that levels of PD-1 or PD-L1 in plasma-derived exosomes vary broadly in different cancer patients (16, 18). The development of a quantitative method for the measurement of these exosome-bound checkpoint molecules allowed us to address their role(s) in cancer-related immune suppression and potentially also in disease progression. We, therefore, evaluated the possibility that PD-L1, which is expressed not only on tumor cells but primarily on antigen-presenting cells (23, 24), is carried on circulating exosomes produced by these various cells and is delivered to activated PD-1$^+$ immune cells, inducing immune checkpoint inhibition. In this context, circulating PD-L1$^+$ exosomes, whether produced by tumor cells or normal cells in the TME, have the potential to modify immune responses and indirectly influence disease activity.

The data we obtained using exosomes isolated from plasma of HNSCC patients consistently and convincingly showed that the frequency of PD-L1$^+$ exosome-carrying beads in plasma as well as relative levels of PD-L1 carried on the exosome surface were associated with disease activity and with clinical stage established for these patients at the time of blood draws. The patients with an excess of PD-L1$^+$ exosomes in plasma had active and more advanced disease than those with low levels of PD-L1$^+$ exosomes. Furthermore, the higher the PD-L1 content of circulating exosomes, the greater was their ability to inhibit activation of CD8$^+$ effector T cells. This dose-dependent suppression of T-cell activity by PD-L1$^+$ exosomes was significantly reduced by anti–PD1-Ab, confirming that exosomes drive PD-1/PD-L1 signaling in responder T cells. These results are consistent with our previous findings of exosome-mediated immune suppression in activated T cells (21, 25).

Effects of exosomes on immune cells can be mediated via different mechanisms (26). Internalization of exosomes by recipient cells via endocytosis or phagocytosis is a common mechanism used by various types of cells (27). T lymphocytes only reluctantly take up exosomes, as we have recently demonstrated (28). Instead, T cells interact with exosomes through the receptor–ligand signaling (28). Here, we have confirmed the involvement of the PD-L1–mediated pathway in the downregulation of CD69 surface expression on activated T cells after their coincubation with PD-L1^{high} exosomes. Suppression of T-cell activation was almost completely reversed by preincubating T cells with anti–PD-1 Ab (Fig. 5). Thus, PD-L1 carried on the exosome surface retains its biological activity and effectively signals via its receptor, PD-1, expressed on activated T cells.

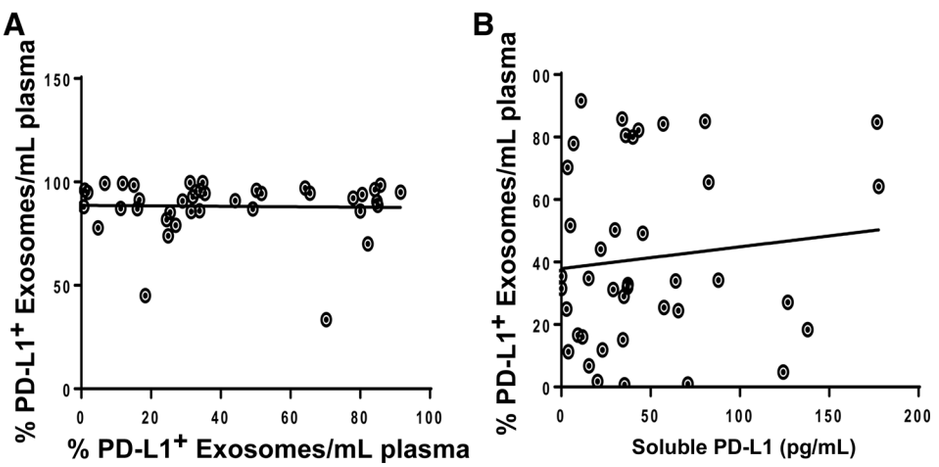

Figure 4.

The percentages of PD-L1$^+$ and PD-1$^+$ exosomes/mL plasma and levels of sPD-L1 in plasma of HNSCC patients. **A,** No correlation between the percentages or RFVs (not shown) of PD-L1$^+$ and PD-1$^+$ exosomes in plasma of HNSCC patients was observed: Spearman correlation at $P = 0.7$, $r = 0.05$. **B,** No correlation between the percentages of PD-L1$^+$ exosomes in patients' plasma and soluble PD-L1; Spearman's correlation at $P = 0.85$, $r = 0.03$.

Downloaded from http://aacrjournals.org/clincancerres/article-pdf/24/4/896/2049722/896.pdf by guest on 21 May 2025

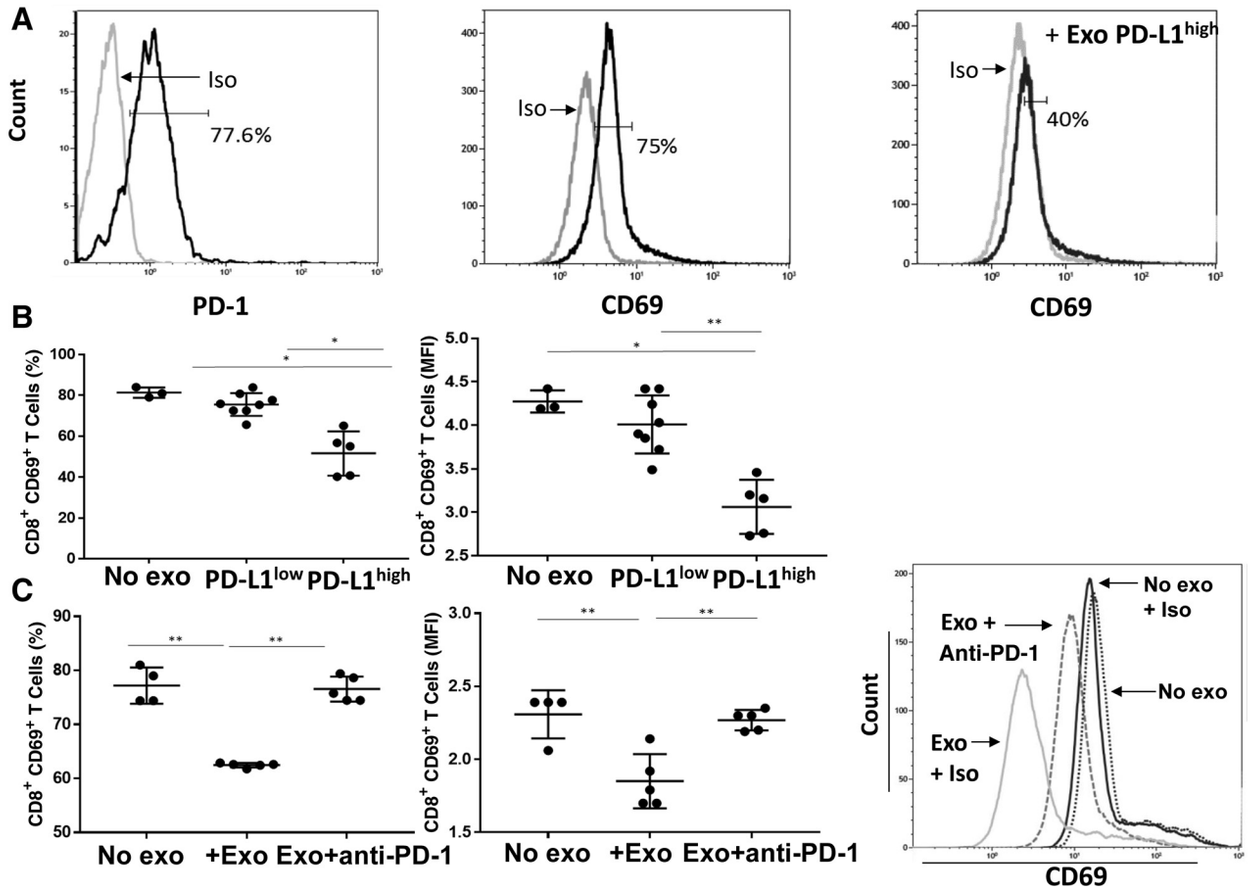

Figure 5.

CD69 and PD-1 expression on activated CD8^{+} T cells and downregulation of CD69 expression by PD-L1^{high} but not by PD-L1^{low} exosomes. **A,** Representative flow cytometry showing expression levels of CD69 or PD-1 on the surface of activated CD8^{+} T cells. Decreasing levels of CD8^{+}CD69^{+} on the surface of T cells coincubated with PD-L1^{high} exosomes. **B,** Downregulation of CD69 expression (% and MFI) on CD8^{+} T cells after coincubation with PD-L1^{high} exosomes. In **C**, blocking of exosome-mediated downregulation of CD69 expression on CD8^{+} T cells by anti-PD-1 Ab. Note that inhibition mediated by PD-L1^{high} exosomes was almost completely reversed (% and MFI) by adding the PD-1 inhibitor. *, $P < 0.05$; **, $P < 0.005$.

Expression of PD-L1 on tumor cells has been correlated with poor outcome to therapy with immune checkpoint inhibitors in various human cancers (29, 30). However, the impact of PD-L1 on response to immunotherapy and outcome is still controversial, with some reports linking PD-L1 expression to better rather than poor responses (31, 32). Similar controversy exists with respect to PD-1 checkpoint expression on immune cells in the TME (33, 34). This study of PD-L1^{+} and PD-1^{+} exosomes in HNSCC did not include patients treated with immune checkpoint inhibitors; thus, we could not consider the impact of PD-L1^{+} or PD-1^{+} exosomes on responses to immunotherapy. We are currently evaluating pre/post-therapy changes in PD-L1^{+} exosomes in HNC patients. Here, we asked whether PD-L1 carried by exosomes has an impact on functions of immune cells and thus, indirectly, on disease activity. We observed a highly significant positive association between the high PD-L1 cargo of circulating exosomes and clinicopathologic disease markers such as the evidence of advancing disease, the high tumor stage and the lymph node involvement. In contrast, PD-1 levels on exosomes while consistently elevated in HNSCC did not correlate with the clinicopathologic patient profiles. This absence of correlation for PD-1^{+} exosomes likely reflects the high receptor occupancy and engagement in HNC cancer. The data suggest that exosomal PD-L1, but not exosomal PD-1, is the clinically relevant variable with the potentially informative predictive value.

In contrast with exosome-bound PD-L1, soluble PD-L1 (sPD-L1) levels in HNSCC patients' plasma did not associate with the clinicopathologic findings in these patients. Serum/plasma PD-L1 levels were evaluated in several previous studies with inconsistent results (35–37). A more recent study indicates that in patients with malignant melanoma treated with immune checkpoint inhibitors, sPD-L1 was shown to predict outcome for a subgroup of patients (38). Ours is the first study that compared the surface PD-L1 cargo in exosomes with sPD-L1 levels in patients' plasma. Interestingly, there was no correlation between the frequency of PD-L1^{+} exosomes and levels of sPD-L1 (Fig. 4B). This might be due to greater stability of the membrane-tethered PD-L1 relative to its soluble counterpart. Alternatively, cellular production and release of sPD-L1 from cells is likely to be independent from the complex packaging machinery responsible for the exosome biogenesis in the parent cells (39). It is perhaps this origin from the endosomal compartment that allows exosomes to

Downloaded from http://aacrjournals.org/clincancerres/article-pdf/24/4/896/2049722/896.pdf by guest on 21 May 2025

mimic the molecular content of PD-L1–producing parent cells and serve as a more reliable biomarker of immune dysfunction.

Our results demonstrating the presence of functional and thus clinically relevant PD-L1 on the surface of exosomes isolated from plasma of patients with cancer emphasizes the emerging importance of exosomes in antitumor immunity and their role as promising future biomarkers of tumor progression. Nevertheless, further studies with larger patient cohorts involving pre/post therapy assessments of PD-L1 and PD-1 on exosomes are needed to validate their potential role as bona fide disease biomarkers.

Disclosure of Potential Conflicts of Interest

No potential conflicts of interest were disclosed.

Authors' Contributions

Conception and design: T.L. Whiteside
Development of methodology: M.-N. Theodoraki, S.S. Yerneni, T.L. Whiteside
Acquisition of data (provided animals, acquired and managed patients, provided facilities, etc.): M.-N. Theodoraki, T.L. Whiteside
Analysis and interpretation of data (e.g., statistical analysis, biostatistics, computational analysis): M.-N. Theodoraki, S.S. Yerneni, W.E. Gooding, T.L. Whiteside
Writing, review, and/or revision of the manuscript: M.-N. Theodoraki, T.K. Hoffmann, W.E. Gooding, T.L. Whiteside
Administrative, technical, or material support (i.e., reporting or organizing data, constructing databases): T.K. Hoffmann, T.L. Whiteside
Study supervision: T.L. Whiteside

Acknowledgments

This work has been supported in part by NIH grants RO-1 CA168628 and R21-CA204644 (to T.L. Whiteside) and by the Deutsche Forschungsgemeinschaft (to M.-N. Theodoraki; research fellowship # TH 2172/1-1).

The costs of publication of this article were defrayed in part by the payment of page charges. This article must therefore be hereby marked *advertisement* in accordance with 18 U.S.C. Section 1734 solely to indicate this fact.

Received September 12, 2017; revised October 25, 2017; accepted December 6, 2017; published OnlineFirst December 12, 2017.

References

1. Whiteside TL. Head and neck carcinoma immunotherapy: facts and hopes. Clin Cancer Res 2017 July 27. [Epub ahead of print].
2. Ferris RL, Whiteside TL, Ferrone S. Immune escape associated with functional defects in antigen-processing machinery in head and neck cancer. Clin Cancer Res 2006;12:3890–5.
3. Bergmann C, Strauss L, Zeidler R, Lang S, Whiteside TL. Expansion of human T regulatory type 1 cells in the microenvironment of cyclooxygenase 2 overexpressing head and neck squamous cell carcinoma. Cancer Res 2007;67:8865–73.
4. Forastiere AA, Zhang Q, Weber RS, Maor MH, Goepfert H, Pajak TF, et al. Long-term results of RTOG 91–11: a comparison of three nonsurgical treatment strategies to preserve the larynx in patients with locally advanced larynx cancer. J Clin Oncol 2013;31:845–52.
5. Chikuma S. Basics of PD-1 in self-tolerance, infection, and cancer immunity. Int J Clin Oncol 2016;21:448–55.
6. Ahmadzadeh M, Johnson LA, Heemskerk B, Wunderlich JR, Dudley ME, White DE, et al. Tumor antigen-specific CD8 T cells infiltrating the tumor express high levels of PD-1 and are functionally impaired. Blood 2009;114:1537–44.
7. Latchman Y, Wood CR, Chernova T, Chaudhary D, Borde M, Chernova I, et al. PD-L2 is a second ligand for PD-1 and inhibits T cell activation. Nat Immunol 2001;2:261–8.
8. Wang X, Teng F, Kong L, Yu J. PD-L1 expression in human cancers and its association with clinical outcomes. Onco Targets Ther 2016;9:5023–39.
9. Topalian SL, Drake CG, Pardoll DM. Immune checkpoint blockade: a common denominator approach to cancer therapy. Cancer Cell 2015;27:450–61.
10. Brahmer JR, Drake CG, Wollner I, Powderly JD, Picus J, Sharfman WH, et al. Phase I study of single-agent anti-programmed death-1 (MDX-1106) in refractory solid tumors: safety, clinical activity, pharmacodynamics, and immunologic correlates. J Clin Oncol 2010;28:3167–75.
11. Ferris RL, Blumenschein G Jr., Fayette J, Guigay J, Colevas AD, Licitra L, et al. Nivolumab for recurrent squamous-cell carcinoma of the head and neck. N Engl J Med 2016;375:1856–67.
12. Ribas A, Hamid O, Daud A, Hodi FS, Wolchok JD, Kefford R, et al. Association of pembrolizumab with tumor response and survival among patients with advanced melanoma. JAMA 2016;315:1600–9.
13. Becker A, Thakur BK, Weiss JM, Kim HS, Peinado H, Lyden D. Extracellular vesicles in cancer: cell-to-cell mediators of metastasis. Cancer Cell 2016;30:836–48.
14. Abels ER, Breakefield XO. Introduction to extracellular vesicles: biogenesis, RNA cargo selection, content, release, and uptake. Cell Mol Neurobiol 2016;36:301–12.
15. Whiteside TL. Tumor-derived exosomes and their role in cancer progression. Adv Clin Chem 2016;74:103–41.
16. Ludwig S, Floros T, Theodoraki MN, Hong CS, Jackson EK, Lang S, et al. Suppression of lymphocyte functions by plasma exosomes correlates with disease activity in patients with head and neck cancer. Clin Cancer Res 2017;23:4843–54.
17. Whiteside TL. Exosomes and tumor-mediated immune suppression. J Clin Invest 2016;126:1216–23.
18. Hong CS, Funk S, Muller L, Boyiadzis M, Whiteside TL. Isolation of biologically active and morphologically intact exosomes from plasma of patients with cancer. J Extracell Vesicles 2016;5:29289.
19. Morales-Kastresana A, Jones JC. Flow cytometric analysis of extracellular vesicles. Methods Mol Biol 2017;1545:215–25.
20. Schuler PJ, Schilling B, Harasymczuk M, Hoffmann TK, Johnson J, Lang S, et al. Phenotypic and functional characteristics of CD4+ CD39+ FOXP3+ and CD4+ CD39+ FOXP3neg T-cell subsets in cancer patients. Eur J Immunol 2012;42:1876–85.
21. Muller L, Mitsuhashi M, Simms P, Gooding WE, Whiteside TL. Tumor-derived exosomes regulate expression of immune function-related genes in human T cell subsets. Sci Rep 2016;6:20254.
22. Risso A, Smilovich D, Capra MC, Baldissarro I, Yan G, Bargellesi A, et al. CD69 in resting and activated T lymphocytes. Its association with a GTP binding protein and biochemical requirements for its expression. J Immunol 1991;146:4105–14.
23. Dong H, Strome SE, Salomao DR, Tamura H, Hirano F, Flies DB, et al. Tumor-associated B7-H1 promotes T-cell apoptosis: a potential mechanism of immune evasion. Nat Med 2002;8:793–800.
24. Keir ME, Liang SC, Guleria I, Latchman YE, Qipo A, Albacker LA, et al. Tissue expression of PD-L1 mediates peripheral T cell tolerance. J Exp Med 2006;203:883–95.
25. Wieckowski EU, Visus C, Szajnik M, Szczepanski MJ, Storkus WJ, Whiteside TL. Tumor-derived microvesicles promote regulatory T cell expansion and induce apoptosis in tumor-reactive activated CD8+ T lymphocytes. J Immunol 2009;183:3720–30.
26. Mulcahy LA, Pink RC, Carter DR. Routes and mechanisms of extracellular vesicle uptake. J Extracell Vesicles 2014;3:24641.
27. Feng D, Zhao WL, Ye YY, Bai XC, Liu RQ, Chang LF, et al. Cellular internalization of exosomes occurs through phagocytosis. Traffic 2010;11:675–87.
28. Muller L, Simms P, Hong CS, Nishimura MI, Jackson EK, Watkins SC, et al. Human tumor-derived exosomes (TEX) regulate Treg functions via cell surface signaling rather than uptake mechanisms. OncoImmunology 2017;6:e1261243.

Downloaded from http://aacrjournals.org/clincancerres/article-pdf/24/4/896/2049722/896.pdf by guest on 21 May 2025

29. Huang Y, Zhang SD, McCrudden C, Chan KW, Lin Y, Kwok HF. The prognostic significance of PD-L1 in bladder cancer. Oncol Rep 2015; 33:3075–84.
30. Muller T, Fay S, Vieira RP, Karmouty-Quintana H, Cicko S, Ayata K, et al. The purinergic receptor subtype P2Y2 mediates chemotaxis of neutrophils and fibroblasts in fibrotic lung disease. Oncotarget 2017;8:35962–72.
31. Kluger HM, Zito CR, Turcu G, Baine MK, Zhang H, Adeniran A, et al. PD-L1 studies across tumor types, its differential expression and predictive value in patients treated with immune checkpoint inhibitors. Clin Cancer Res 2017;23:4270–9.
32. Patel SP, Kurzrock R. PD-L1 expression as a predictive biomarker in cancer immunotherapy. Mol Cancer Ther 2015;14:847–56.
33. Thompson RH, Dong H, Lohse CM, Leibovich BC, Blute ML, Cheville JC, et al. PD-1 is expressed by tumor-infiltrating immune cells and is associated with poor outcome for patients with renal cell carcinoma. Clin Cancer Res 2007;13:1757–61.
34. Kim MY, Koh J, Kim S, Go H, Jeon YK, Chung DH. Clinicopathological analysis of PD-L1 and PD-L2 expression in pulmonary squamous cell carcinoma: comparison with tumor-infiltrating T cells and the status of oncogenic drivers. Lung Cancer 2015;88:24–33.
35. Zhang J, Gao J, Li Y, Nie J, Dai L, Hu W, et al. Circulating PD-L1 in NSCLC patients and the correlation between the level of PD-L1 expression and the clinical characteristics. Thorac Cancer 2015;6:534–8.
36. Chatterjee J, Dai W, Aziz NHA, Teo PY, Wahba J, Phelps DL, et al. Clinical use of programmed cell death-1 and its ligand expression as discriminatory and predictive markers in ovarian cancer. Clin Cancer Res 2017;23:3453–60.
37. Okuma Y, Hosomi Y, Nakahara Y, Watanabe K, Sagawa Y, Homma S. High plasma levels of soluble programmed cell death ligand 1 are prognostic for reduced survival in advanced lung cancer. Lung Cancer 2017;104:1–6.
38. Zhou J, Mahoney KM, Giobbie-Hurder A, Zhao F, Lee S, Liao X, et al. Soluble PD-L1 as a biomarker in malignant melanoma treated with checkpoint blockade. Cancer Immunol Res 2017;5:480–92.
39. Colombo M, Moita C, van Niel G, Kowal J, Vigneron J, Benaroch P, et al. Analysis of ESCRT functions in exosome biogenesis, composition and secretion highlights the heterogeneity of extracellular vesicles. J Cell Sci 2013;126:5553–65.

Downloaded from http://aacrjournals.org/clincancerres/article-pdf/24/4/896/2049722/896.pdf by guest on 21 May 2025